American Journal of Interdisciplinary Research and Development
ISSN Online: 2771-8948
Website: www.ajird.journalspark.org
Volume 08, Sep., 2022

SPECTRUM-SHARED CELLULAR INTERNET-OF-THINGS (5G) COMMUNICATIONS THROUGH RF ENERGY HARVESTING & TRANSFER

Wijdan Noaman Marzoog Al Mukhtar
Bachelor's degree, Department Computer Science College of Science for Women University of Babylon, Babyl, Iraq.
Master's degree, Department of Computer Engineering and Information Technology Razi University , Kermanshah , Iran .
wijdanalmokhtar@gmail.com

Haroon Rashid Hammood Al Dallal
Bachelor's degree, Department of Communications Al-Furat Al-Awsat Technical University, Najaf, Iraq.
Master's degree, Department of Information Technology and Communication Systems , Saratov State Technical University , Saratov , Russia .
haroonra1994@gmail.com

Abstract
In this research, we provide a 5G-capable IoT infrastructure that optimizes spectrum and electricity. It uses energy harvesting or energy transfer to minimize its impact on the cellular network's performance. The Internet of Things network comprises sensor nodes and a power-efficient cluster head that repurposes unused portions of the cellular frequency spectrum. The cluster leader is in charge of spectrum utilization, random sequencing of sensor nodes, or scheduling downtime for energy transfer. The cellular communication and transferred power from the cluster are converted into RF energy, which the sensor nodes then use. As long as the sensors have power, they will send the data they have acquired at the appointed time. Spectrum supply, energy availability, information transfer, and energy transfer all come into play as a result of the interaction between both the cellular and IoT network. This study demonstrates that, for a given amount of cellular traffic, an increase in the number of devices in the network leads to a multi-user gain due to the IoT network's increased utilization and the broadcast aspect of the transfer of energy. The findings shed light on the kind of Internet of Things applications that might be feasible under various operational regimes.

Keywords: Energy harvesting, energy transfer, cellular IoT, and 5G systems.

Introduction

Other forms of communication exist besides the more conventional human-to-human and human-to-machine channels, a new phenomenon named the Internet of Things (IoT) [1] is becoming increasingly noticeable, in which the machines in our environment communicate with each other through minimal human involvement and the ultimate goal of improving our quality of life. In this model, inexpensive sensors, actuators, and related devices work together to generate, exchange, process and act on data in pursuit of a common purpose. Health [2], smart metering [3], traffic control [4], intelligent buildings [5], agroecosystems [6], environmental control [7], etc., are only a few of the many potential uses.

Broad area IoT systems can't function without cellular technology [8]. Upcoming 3GPP releases aim to improve cellular IoT communications to meet their specific needs in energy, spectrum and signaling overhead. In particular, widespread rollouts of low-throughput, low-power-consumption devices are expected to rely on new low-complexity, narrowband radio technologies [9].

The goal of this work is to create a novel design for a cellular IoT scheme that is ready for the 5G future, one that achieves efficiency in both spectra (through opportunistic recycling of the energy through an energy harvesting system) and the electromagnetic spectrum (from cells) of acoustic signal transmission or RF power injection). A system like this makes it easy to see the trade-offs that must be made to maximize efficiency in terms of spectrum sharing, available energy, data, or energy transfer. To predict potential operational modes where such networks can function, we plan to create a mathematical model that can extensively explore these trade-offs. It's possible that the combined traffic from thousands of sensors used in wide-area cellular IoT applications won't be enough to justify the cost of dedicated cellular services. For instance, during the mooring of the climate system, every sensor may report only a tiny amount of data for a long time, say an hour and a full day, but then report everything at once. To extrapolate, for instance, the temperature/humidity ratios for all locations, it may be necessary to query a representative selection of these devices using the gathered data. As a result, this paper presents an Internet-of-Things system that strategically uses empty airwaves while cell phones aren't in use [10].

Massive IoT deployments have energy as a critical design constraint. A green, relatively low-power architecture may be required for such networks even though individual nodes' energy usage may be low. Moreover, it is planned that the vast majority of these gadgets will be installed in permanent locations outdoors. That's why it's crucial to devise a method of everlasting operation that doesn't rely on external power sources or periodic battery swapping. Interest in energy collecting systems [11], [12], [13] has grown in response to these needs. Mechanical, electrical, thermal, solar, physiological, etc., energy can all be tapped into. Radiofrequency (RF) energy harvesting is a topic that has been discussed in recent years [14], [15]. Even though the

energy gained by RF harvesting is substantially lower than other sources like solar energy, its portability and usability in any environment at any time of day or night are significant benefits. More effective ways for collecting RF energy are expected to be developed soon [15], [16]. This paper, therefore, proposes a system consisting of cellular IoT nodes capable of either drawing RF power from nearby cellular signals or injecting RF power into the grid in times of need.

The planned Internet of Things network uses two distinct types of nodes. An army of cheap and efficient sensor nodes makes up most of the Internet of Things (SN). Cluster heads (CLH) are the other variety; they're more robust, manage the sensor nodes, and handle the RF power transfer procedures discussed in detail below. A real-world IoT solution may have multiple clusters, each with a cluster head. The focus of this research is on one such group.

Time and frequency slots for the cellular network coexist with the IoT network. Examples of such systems include OFDM and SC-FDM, which LTE networks use in the uplink and downlink, respectively. Continued work is being put into standardizing the 5G wireless connectivity, also known as 5G New Radio or 5G NX [17]. In theory, the 5G NX would be constructed with an improved, flexible air interface similar to OFDM. The radio assets are then time and frequency slotted, a repeated process for LTE and 5G. Cellular resource blocks are the time and frequency intervals so created. At each transmit period, the cellular ground station distributes these spectrum resources to several users or regulates traffic data (TTI). It is assumed that the TTIs of the wireless network and the time slot architecture of the IoT connection coincide. Given the massive complexity but also power consumption increases, it is not expected that sensor networks will employ the same communications as the wireless network. We propose that SNs' radios are tuned to a fixed, limited frequency, for instance, covering a few wireless accessible spectral bands, to interact with the clusters via a thin physical layer designed for low power consumption, as per the most up-to-date IoT standards from 3GPP [9].

This is how the projected IoT network will function. The cellular network, at each TTI, makes independent use of the IoT network's allotted cellular resource blocks. Spectrum detection at the tuned frequency is performed at each TTI by the IoT cluster head. It has been discovered that the IoT network makes opportunistic use of this frequency whenever the cell connection is not using it. When a window of opportunity presents itself, the CLH must determine whether to use it to send RF energy to the SNs or receive data from them. Whenever an information exchange is to be made, the CLH will pick an SN at random for scheduling purposes. But if the choice is to transfer energy, the CLH will send signals for Rf power collection. When not actively transmitting data, SNs conduct RF energy harvest by absorbing either the natural cellular network signals or the signal supplied by the CLH. In this third section, we delve into the intricate interplay among sensing, energy harvesting, or data/energy

transfer operations; cellular or IoT data movement models; signaling between the CLH with SNs; retransmission due to collisions; and more.

Through spectrum collaboration with the cellular network or energy harvesting and transmission, our work provides the first energy- or spectrum-efficient 5G Internet of Things network, setting it apart from earlier 5G IoT models. Here, we focus on a framework wherein the RF waves power the sensor nodes. Cluster heads are proposed for usage in IoT networks for management and, where necessary, power transmission. The energy for Internet of Things devices is provided by either the cell link or the cluster's base station. The availability of airwaves for sensor network transfer is sufficient along a generally idle path, but more energy transfer is required for a feasible operation when cell traffic is heavy. In this research, we not only develop a more precise mathematical model to characterize cellular and IoT traffic than earlier work in the research, but we also conduct extensive experiments to examine these tradeoffs. We demonstrate that, for a given amount of cellular traffic, a more significant number of sensors leads to greater utilization of the IoT network and, ultimately, a benefit for multiple users because energy is transferred throughout the network in a broadcast fashion.

It's been said that 5G will make the Internet available to anything and everything. By 2021, there will likely be over 28 billion linked devices, with over 15 million connections between machines [18]. This makes providing connectivity for the Internet of Things (IoT) a top priority for the 5G network [19]. Self-sufficiency in network operation is a cornerstone of the Internet of Things [20]. In this regard, energy harvesting has been gaining popularity as a viable strategy [20, 21]. In this research, we propose a spectrum-sharing Internet of Things network that harvests and transmits energy to coexist with other 5G services.

There has been a lot of discussion in the scientific literature about RF energy harvesting systems lately. Depending on the scenario, a realistic node can only interpret information or gather RF signal energy, but predictive control rules must be created for each circumstance [22, 23]. A user equipment (SU) with infinite backlog traffic rather than a simple energy usage concept needs to execute error-free sensing and calculate the ideal schedule for balancing data transmissions, spectral measurements, and energy harvesting in a perceptual radio network, as proposed by Yin et al. [24]. Using a transmitter, decoder, and energy harvester, Zhang & Ho [25] determine the rate-energy areas for a MIMO system. By taking into account, the SU transmit power, and SU density in a particular area, Lee et al. [16] use stochastic geometry to optimize the geographical SU throughput. It is hypothesized in the research that such a secondary user (SU) can harvest energy from a primary user (PU) if the SU is physically close enough to the PU. Zheng et al. [26] investigate a system in which SUs with energy collecting capabilities transmit to Pus to improve the latter's efficiency in exchange for additional spectrum access.

Ku et al. [27] optimize the solar energy sensor network's transmission range using Markov decision techniques to increase the network throughput. Chan et al. [28] use the 4-D continuous Markov chains model with adaptive load cycling to provide everlasting operations with QoS supply in a regenerative braking sensor network. Similar to busy/idle models, the channel used in this paper can be in one of two states. However, the idea of opportunistic access is disregarded in both of these papers. See [29], [30] for an analysis of a system wherein SUs harvest Rf energy from PU signals and then use this power to generate optimal SU channel access policies based on a mixture of Markov decision processes with some of the states hidden from view. The incoming flow is presumed to follow a Bernoulli distribution. The SUs in the slotted system considered in [31] is in charge of energy harvesting, spectrum detection, and transmission, one after the other. Energy detection is the interactive basis of spectrum sensing. Together, the optimal sensing time, fusion rule, or sensing threshold are what makes the difference when it comes to maximizing SU throughput. RF energy transfer is not assumed here.

Kim and Hwang [32] consider an N SU, M channel cognitive radio network. Packets arrive at Pus and SUs according to Bernoulli processes or are queued up for infinite amounts of time. When the queues of the Pus are not empty, the Pus will transmit on their designated channels. A channel is chosen randomly, imperfect sensing is performed, and if the route is accessible, the SUs begin transmitting. While this paper's model is comparable to ours, it does not consider energy collecting, transmission, or SU battery life.

Another article, [33], uses a 2-dimensional constant Markov chain model deriving from the premise of decoupled SU queues to examine the SU queue PMF or the packet waiting times under the assumption of perfect channel sensing. The same authors, in [34], generalize their analysis to multi-interface setups with imperfect sensing. The concepts of energy harvesting and consumption are ignored in both works.

When compared to the prior literature, this work introduces numerous new ideas. To start, it presents the first model for a spectrum- and energy-efficient 5G wireless IoT network by proposing the reuse of a portion of the cellular spectrum and the collection of both ubiquitous cellular RF signals and the injection of RF energy to increase energy efficiency. Second, a Markov Chain model is used to analyze the resulting trade-offs in light of a more realistic scenario than that presented in the prior literature. This scenario assumes that the cellular network uses retransmissions, that both networks queue incoming packets, that incoming traffic is bursty rather than continuous, and that spectrum utilization is imperfect.

American Journal of Interdisciplinary Research and Development
ISSN Online: 2771-8948
Website: www.ajird.journalspark.org
Volume 08, Sep., 2022

2.Method

PROPOSED MODEL OF THE SYSTEM

Figure 1 depicts the proposed topology for 5G cellular IoT networks, within which the IoT networks coexist with the harvesting or transmitting IoT network. Technology for cellular networks is similar to orthogonal frequency division multiplexings (OFDM). Without considering the IoT network, the mobile phone base station distributes users and prioritizes traffic over the available bandwidth in this sub-band at each TTI. We can extrapolate that this means a TTI will last for T s. A typical TTI in an LTE network would be one millisecond or one subframe time. A fluctuating TTI ratio is predicted for 5G NX [17]. To avoid interference with cellular modems, the proposed IoT network works in time slots that are in sync also with the TTI design of the mobile network.

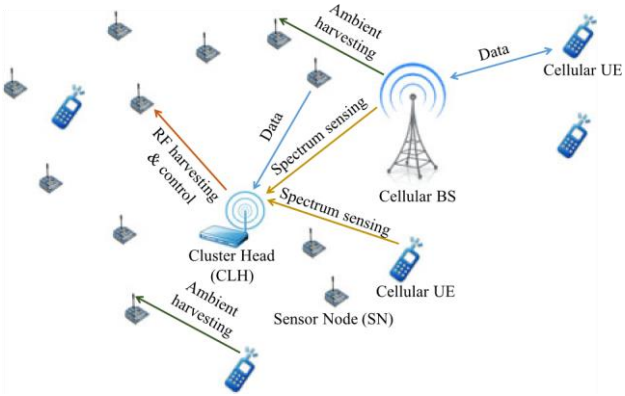

Fig. 1. Conceptualized energy and frequency-sharing

A cluster head (CLH) or Ns sensor node makes up an Internet of Things network (SNs). The CLH is highly effective and wired to a steady supply of power. A real-world IoT solution may have multiple clusters within each cluster head. In this study, we concentrate on one such subset. When an IoT network first goes live, the CLH syncs up with the TTI design of the wireless network by listening. For the IoT to function, the CLH must identify the windowed cellular sub-band spectrum and coordinate the transmission of sensor nodes to coincide with these windows to gather their sensor data and provide wireless power and data to the nodes. It is expected that the CLH uses a wired connection or a different band, such as 802.11, to send the data collected to an application database.

Sensor networks are less potent than others, but there are many of them. They are powered by small batteries and have strict power limits. These nodes are responsible for data collection and storage of sensory information. If they have the information and the power to transmit it, they will transmit for the entire slot period when the

cluster head schedules it. In either case, they resort to energy harvesting, which can happen either via a broadcast from the cell site or UEs.

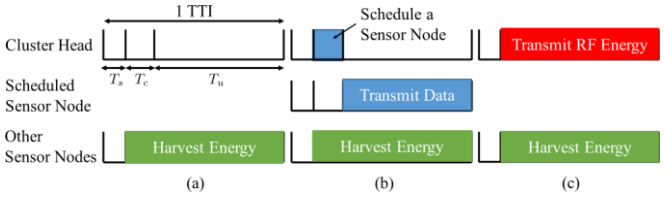

Fig 2: Structure of LOT networks

The cellular band sub-band for Internet of Things data transmission is also used for the RF energy transfer. The CLH chooses whether this empty sub-band will be used for power or data transmission. The OFDM-like signals discussed above, for instance, might also be utilized to transport RF energy. Because of this, SNs can gather either signal with the same antenna and electronics. If this assumption turns out to be false in the real world, Internet of Things devices may be built with separate cellular signals and RF transmission collecting circuitry. Both harvesting strategies relied on a capacitor near the sensor nodes' receiving antenna to store the generated electrons [15].

Figure 2 depicts the slot architecture of the wireless IoT network. The CLH performs a channel sense for cellular communication for Ts seconds at the start of each slot. This research does not attempt to predict how long Ts will take. It depends on various variables beyond our control, including signal-to-noise ratio (SNR), sensing technique employed, computational resources available in the CLH, etc. Based on this, we estimate that Ts is less than 1 TTI. For the paper's proposed cellular IoT and 5G coexistence to work, spectrum sensing must evolve to accommodate the longer slot lengths of 5G networks.

If the CLH determines that the channel is in use, it will do nothing until the slot time expires. See Fig. 2a for visual evidence. Whenever an SN is planned, it is planned uniformly at random; if it is decided to schedule an SN, then the likelihood that any given SN will be scheduled is N1s. To maintain the unidirectional nature of the coordination communications between the CLH and SNs.

At a time coordinated to be Tc, the schedule decision is sent to the SN. CLH waits for the scheduled SN's transmission during the utilization duration Tu 14 T Ts Tc. When an SN has data or enough energy to transmit, it listens for a scheduling message and sends it. Without any other means of obtaining energy, an SN will resort to harvesting. The harvesting of an unscheduled SN, and perhaps a scheduled SN without sufficient data or energy to perform RF transmission, is depicted in Figures 2a and 2b. This occurs even though the CLH is not actively transmitting. This could happen if the CLH either successfully detects the cellular signal or fails to do so and instead plans to send

out another SN. In the above-described channel access paradigm, the coordinating messages are assumed to flow solely in one way, from CLH to SNs. The limited power from the SNS made this decision necessary, as it is impossible to anticipate all SN units to communicate routinely. Our work in Section 6 demonstrates that increasing the number of SNs used effectively addresses this deficiency.

When a cellular packet is lost in transit, the hybrid ARQ technique utilized by modern wireless networks causes it to be reissued up to N+1 times. However, the IoT network as a whole can handle packet loss without affecting the functionality of the application. To create a temperature, humidity, etc., map, a climate monitoring application, for example, typically interpolates data from numerous sensors. It is common practice to build redundancy and tolerance for data gaps in such procedures. Additions to the SNs' functionality, such as ARQ, would raise their overall complexity and power consumption. As a result, SNs only employ forward error correction and do not retransmit lost packets.

3.CELLULAR Or IoT TRAFFIC MARKOV CHAIN MODELING

The above model suggests a trade-off between transmission time and harvesting time: allocating more excellent harvesting time results in more energy harvested but fewer spectrum possibilities for transmissions. It's possible that there won't be enough juice to go around if much time is spent on broadcasts. This research aims, in part, to evaluate this trade-off. Markov chains, which describe the cellular above or IoT traffic models, are used for the analysis. We make the following presumptions to begin building our models.

It is assumed that the channel sensing is not flawless. Missed detections occur with probability pMD when the CLH wrongly determines that the cellular subchannel is empty. Similarly, a false alarm occurs when the CLH erroneously determines that the sub-channel is busy when it is not. This occurs with a probability pFA for each slot individually. The analysis's pMD and pFA values can be adjusted to accommodate the specifics of the CLH's sensing technique. Using cyclo-stationary sensing rather than energy sensing, for instance, would result in lower pMD and pFA [35]. In the most extreme case, a CLH capable of decoding scheduled information broadcast by the cellular BS would be invaluable. Without changing the scope of our research, let us assume that pMD = PFA = 0; in this scenario. However, even in this instance, the scheduled SN might not get the scheduling information right a small percentage of the time. This amounts to a false report in practice. The CLH may also wish to repurpose the channels once [36].

When the CLH fails to identify a cellular signal but orders an SN to transmit (since it has the necessary data or enough energy to do so), the SN and the cellular packet will collide, and both will be lost. There is a loss of the cellular package when the CLH carries out a missed detection or subsequent RF energy transfer. The system model for

this scenario allows for the retransmission of cellular packets up to N 1. In contrast, the sensor nodes employ forward error correction and do not retransmit lost packets. In this work, we adopt the on-off process commonly employed in literature for modeling bursty traffic [37, 38, 39] as the source of the aggregate wireless incoming packet traffic. If there wasn't a cellular packet in this slot, then within the next slot is the most likely time for a burst's leading packet to arrive.

If a packet has been received in this slot, then there is a b% chance that there won't be any further packets arriving in the next slot. Suppose it arrives during the transmission of an existing packet. If there is already too much traffic in the queue, the new packet will be discarded. Once a packet has been successfully sent, or the maximum number of attempts has been achieved, the next packet in the queue will be sent during the next transmission slot. Note that we assume a unified queue and incoming traffic for the downlink and downlink, as a base station plans wireless transmissions. An alternative method of characterizing the spikey incoming traffic is to use a semi-Markov model. Still, we follow the prior research and utilize an on-off Markov chain instead. Our approach, in contrast to the simple on/off model, accounts for retransmissions and queueing of incoming packets, which results in more realistic transmitted traffic.

Data packets arriving at an SN are modeled in an on-off fashion, just as cellular traffic, with a probability of as for packets arriving at the front of the queue and a probability of bs for the conclusion of a burst. It is also expected that each SN uses a queue with a maximum size of S items. As was previously indicated, collisions are not handled by resending packets from the SNs because it is presumed that they use forward error correction.

If the CLH detects an empty channel and chooses to transmit RF energy, all SNs will harvest RF energy during that slot. In the event of a failed detection, RF harvesting continues regardless. There is interference between the cellphone signal and the RF energy signal.

All energy definitions below are about the amount of energy harvested from the surrounding environment in a single storage slot. It is assumed that each SN collects L energy units during the time slot devoted to RF transmission. This is the same as supposing that the amount of energy collected equals L times the amount of energy harvested from the surrounding environment. If an SN has data to communicate, is on the transmission schedule, and has enough energy, it will send a packet. Let's say, for the sake of argument, that the SN expands K energy units. If an SN is not planned to transmit over radio frequency (RF) or if it lacks the necessary energy or data to send, it will resort to ambient harvesting. One unit of energy can be harvested from the ambient environment if the wireless connection is transmitting simultaneously. Keep in mind that even if an SN gets slated for transmission, other SN may still undertake ambient harvesting if this occurred after the CLH did not initially detect the SN. Let's

assume, for the sake of argument, that an SN has a battery system capable of a B unit. Assume K, L, or B are all relatively prime. If not all natural frequencies are fundamental to ambient collecting energy, a lower quantization level can be defined without compromising generality.

Furthermore, we define multiple harvested energy levels to account for the difference in harvested energy levels caused by varying signal intensity. In the case of RF energy transmission, for instance, we can suppose that an SN will collect energy proportional to one of L1, L2,..., Lh units, with corresponding probabilities. Our Markov Chain simulations below will have additional paths thanks to them. We simplify matters by assuming a constant amount of gathered energy across all operations.

4.Decoupling Presumption

Sharing resources like a limited queue, packet retransmission, or RF energy transfer and harvesting from cellular traffic profoundly impact the behaviors of wireless or IoT networks. In the event of collisions brought on by the IoT network's failed detections and subsequent RF or data broadcasts, the wireless connection may resort to retransmissions or queue up its incoming data. The availability of specific ambient harvesting and spectrum possibilities for the IoT network is, in turn, dependent on the transmission activities of the cellular network. Due to their dependence, parameters such as the repetition status or separate assault charges of the data connection and each sensor node, as well as the queue depth and packet entrance processing condition of the wireless network, must be represented by a combined Markov chain. The size of the resultant state space is O(Ns2)MNBS(s), which may be too massive for efficient numerical analysis.

We solved this issue by decomposing the joint Markov chain into two independent chains, one each for the cellular network as well as the SNS. Because of this, instead of evaluating a single massive chain with O'Ns2MNBS' states, we have to analyze two chains, one for the mobile network and one for the Ns identical SN networks. In what follows, I will go into greater depth on these chains or the analysis performed. The underlying assumptions of decoupling are described in more detail below.

In the pioneering work of Bianchi [40], the decoupling assumption is first used to analyze the performance of an 802.11 network with a single cell. An essential (decoupling) premise of this approach is that "the packet collisions risk that all nodes experience is constant and thus the various back-off processes are independent." If we assume that the collision probability is known, we can then calculate the attempt chance for each node, which may then be used to estimate the collision probability. The resulting fixed point equation (FPE) calculates the unknowns in the collision and attempt probability.

Several subsequent articles on the performance monitoring of wireless networks have made use of the decoupling assumption as well as the ensuing FPE approach, such as

[38], [41], and [42]. This has led to an examination of the reasonableness of the assumption in question. Because of this, it has been demonstrated [43]. The reliability of the decoupling assumption is translated into ODE stability as the equilibrium position of this ODE agrees with the equations of Bianchi's FPE. Although it was previously thought that the originality of the FPE solutions implied the validity of the decoupling assumption [44], subsequent work by Cho et al. Along with this, they have introduced a criterion they call "Mild Intensity (MINT)," which they claim implies the ODE's stability. If there are N nodes in the network, then the chance that any given node will attempt stage k of the back-off process will grow as qk=N, where qk is permanent to Qk = 1, and N is the number of nodes. The condition is MINT. By calculating a fractional-order perturbation equation, we can calculate the steady-state probability distribution functions (PMFs) of the detached Markov chains using this hypothesis (FPE).

5.Discussion

The arithmetic characterizes the channel utilization rates of cellular and IoT networks mean values of the ratio of positions with get-through transmissions to the total number of slots over time. Time spent on sensing and coordinating by the IoT network is factored into this definition. To counter this, one option is to adjust IoT usage levels accordingly. Here, we extract the cellular or IoT networks' channel utilization rates. To begin, we will offer an approximate assessment that makes several simplifying assumptions to give readers a sense of the fundamental tradeoffs inherent in the functioning of a cellular IoT system that allows for the transmission and harvesting of RF energy through reactive spectrum sensing.

6.The Use of a Quick Approximation

For a basic system model, calculating cellular and IoT utilization levels is straightforward. Imagine there is an indefinite backlog of SNs in the system. Further, let's presume that the wireless connection attempts to retransmit any packets lost due to a collision until they are delivered successfully. This is the same as supposing that there is limitless demand on the cellular network's queue and that there is no limit on the number of retransmissions that may be made. Without any accidents, the percentage of available bandwidth used by incoming mobile traffic is

QC ¼ a þ b: (11)

Assuming the SNs are eternally behind and have plenty of transmission power, a collision will occur every time the CLH makes a missed detection. Given the probability of collisions, the share of the channel used by the wireless network should be equivalent to

One n a 1

CC ¼ QC Xn¼0ðpMDÞ ¼ a þ b 1 pMD ; (12)

American Journal of Interdisciplinary Research and Development
ISSN Online: 2771-8948
Website: www.ajird.journalspark.org
Volume 08, Sep., 2022

Given that collisions always necessitate retransmissions. It follows that the section of the stream where collisions occur is proportional to

A MD

CX ¼ CC QC ¼ a þ b 1 pMD : (13)

Keep in mind that a portion of CLH RF energy transmission but a portion of collisions are attributable to SN transmissions because the CLH executes RF energy transfer with frequency 11ppwhen it perceives the channel as empty. When the communication modem is down, and the CLH triggers a false warning, the channel is left unusable. Then the unused bandwidth of the channel is proportional to

CI ¼ ð1 CCÞpFA: (14)

When the chain energy transmission channel has a probability of NL and is empty, CLH performs RF1 p in addition to the 1 PCX term above. This means that the CLH's overall channel occupancy for RF transfer of energy is equal to

CRF ¼ ð1 CCÞð1 pFAÞð1 pÞ þð1 PCX : (15) | channel empty ffl{z ffl} |collisions fl{z ffl}

As a result, SNs execute ambient harvesting in the energy gathered from RF transmission in 1 PCX segment of the channel, which is used by the wireless network but does not interfere with the CLH. The energy limitation on the route that SN broadcasts may use is calculated as follows: L times the energy received via ambient harvesting per unit time, where K is the energy spent on transmission.

Use ¼ LCRF þ CCK ð1 pÞCX : (16)

Yet another constraint is imposed by the quantity of available spectrum. To rephrase, if an SN has access to a piece of the channel that has been accurately detected as free & scheduled for SN transmission, then it may use only a fraction of N1s of that portion.

$$U_S^s = \frac{(1 - C_C)(1 - p_{\mathrm{FA}})p}{N_s}. \qquad (17)$$

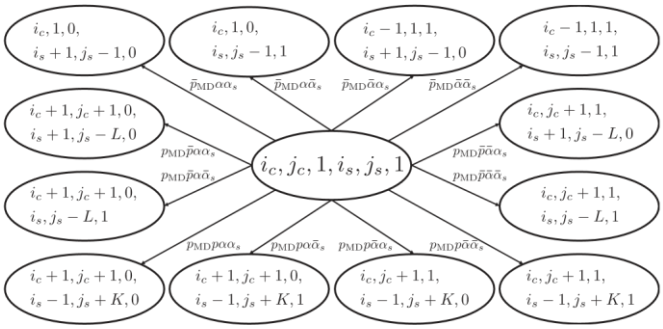

Fig 3: joint Markov process

Changes from the initial state of the joint Markov process are shown in Figure 3. Under these conditions, the wireless network is considered to be sending but not yet at its

maximal number of transmissions N, the SN's battery is assumed to be charged entirely (L js B K), while there is only one SN (0 ic M; 0 is S). As a brevity measure, x is utilized in place of 1 x in the transition probabilities.

The total amount of the channel a single SN uses for broadcasts equals the smaller of these two restrictions. It may be approximated that the utilization level of an IoT network is equal to approx 14 NsminUSe; USS; (18), where Ns is the number of SNs, and USapprox is the fraction of the channel used by all SNs.

Simulations showed that this simplified approximation gets closer to reality as Ns! increases while SN data gathering becomes more bursty (bs! increases). The results, however, show that this is not even close to being a reasonable assumption (Section 6). The whole model is then analyzed, including the effects of non-infinite queues, bursty SN congestion, a wireless network with a limited queue length, a finite total number of packet forwarding for colliding packets, and so on.

7.RESULTS

Here, we compare the outcomes of Monte Carlo simulations with those generated from our thorough model of Markov chains for various system characteristics. The default values for the experimental system parameters are discussed in Section 2 unless otherwise specified. The Numerical Simulations have been run for 1,000,000 iterations of time. Time is an integral part of the simulations. Both the cellular network's packet arrival process and the SNs' arrival processes are simulated, making the total number of simulated packet arrival processes Ns 1. Whether the cellular network's queue is full or empty, if a packet comes within an available time slot, the network will continue to send the packet. If the packet is lost due to interference from an SN transmission, it will be sent again in the following slot. Each packet receives up to N possible tries at transmission. During communications, packets that arrive are queued up. If there are too many packets in the queue, they will be lost.

Initial SN battery capacities are considered to be independent and identically distributed over a range of 120; B for each run. An SN will queue up any incoming packets until it is time and energy-efficient to transmit them. If a packet is lost due to a collision, the SNs won't resend it. When the queues for incoming data are complete, the packets are ignored. An alternative explanation for what happens whenever the SN stack is complete is that the eldest packet in the queue is discarded to make place for a new one, but this may not be the case depending on the type of IoT application being used. The outcomes that follow are unaffected by this. As discussed in Section 3, the CLH and SNs are responsible for sensing, scheduling, transferring RF energy, harvesting energy, and transmitting data. The usage rates of cellular networks and the Internet of Things are determined by dividing the number of positions in which transmissions were victorious by the overall number of modules available for that run. The numbers represent the average usage over 25 separate Monte-Carlo simulations.

The aggregate SN utilization rate is presented for the IoT network. Each simulated usage level has standard deviations substantially less than their respective means. In the results shown below, we show that, as indicated in Section 4.1, for high numbers of sensor nodes and tiny missed detection probability, the Markov chain analyses strongly resemble the Monte-Carlo simulations.

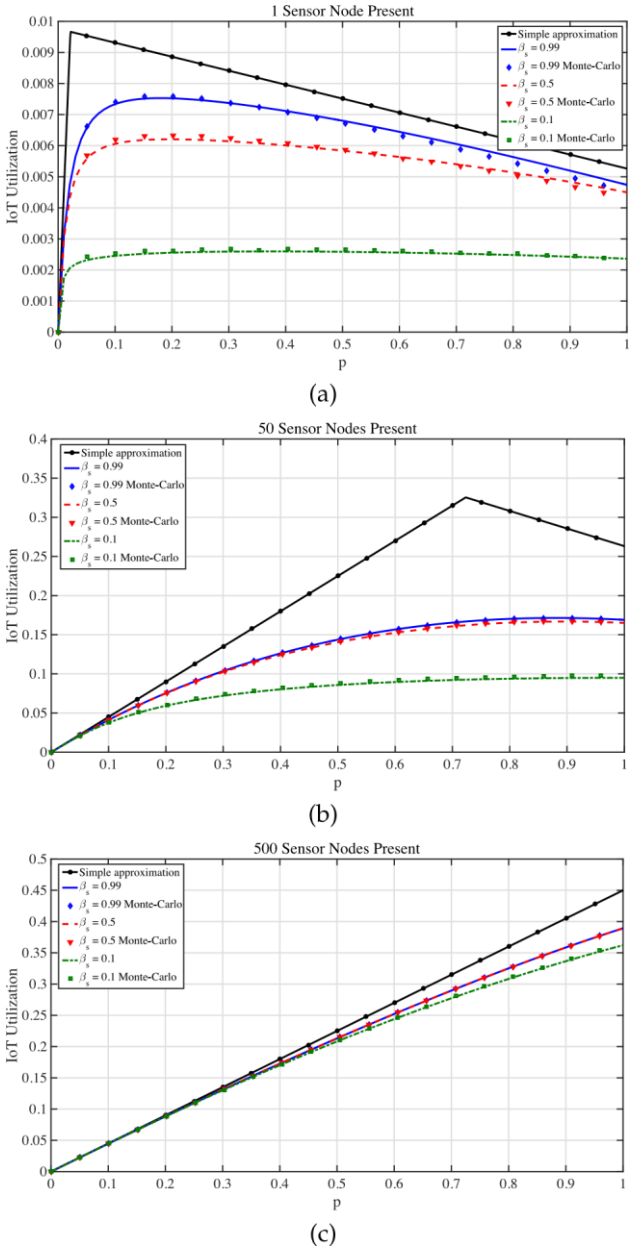

Figure 4: loT network utilization levels

As a first step, we analyze how the probability of SN scheduling, denoted by the symbol p, affects the overall utilization of the Internet of Things (IoT). This is depicted in Fig. 4 for networks with 1, 50, and 500 sensor nodes. Since the proportion of the channel

not filled by the wireless network is mainly utilized to transfer the energy for these probability values, the effectiveness of the IoT systems is limited. On the other hand, if p > p, the available power in the sensor nodes limits how much the IoT can be used. Energy transfer is becoming less common at higher p, leading to lower SN utilizations. Since the sensors are scheduled less, the power generated from atmospheric harvesting is sufficient even if there are a considerable number of detector nodes present, say 500, as in Fig. 4c).

In addition, the figures incorporate the IoT utilization determined by the straightforward approximation presented earlier. Utilization of an Internet of Things network, as discussed above, typically increases with p at first but is ultimately capped by the amount of available spectrum (USS Use in Equation 1). (18). Utilization falls as p increases when power is the limiting element (USS > Use). For a set of SN traffic patterns, it is clear that the simple approximation dramatically exaggerates the amount of time people spend using the Internet of Things. However, as the number of sensors grows, the approximation's accuracy improves. When the amount of sensor nodes within a network is low, we see in the figures that the SN routing process significantly impacts the IoT usage levels. This is because queue overflows happen less frequently with shorter bursts (bigger bs) of SN traffic, resulting in a better utilization rate.

One last thing to mention about Fig. 4 concerns the reliability of the decoupling presumption. The most significant discrepancy between the Markov chain analyses and the Monte Carlo findings occurs when only one SN is present, even though the former closely follows the latter in all graphs. A difference of 50 or 500 SNs is not statistically significant. This coincides with the results of the investigation presented in Section 4.1.

Use of the Internet of Things (IoT) networks as a function of scheduling probability p for bs two f (0,1,5,99)g is shown in Fig. 6. There are (a) exactly one, (b) exactly fifty, and (c) precisely five hundred sensor nodes. The difference between the bs 14 0:99 and bs 14 0:5 curves is too tiny to be seen in (c).

The following plots show the utilization levels for such optimum power transfer strategies, and the efficient scheduling probability, p, is derived numerically for each data point.

Using the example of the deployed sensor nodes, we can examine the cellular, IoT, and total utilization levels in Fig. 5. Our findings show that the use of the IoT network rises in tandem with the number of connected devices. Due to the broadcast aspect of energy transmission, we may see this rise due to a multi-user gain. When more nodes are added to a network, more data is gathered from the surrounding environment and transmitted. While a rise in the network's nodes hurts any particular sensor node's scheduling probability and hence reduces that node's utilization, overall IoT network

utilization rises. An increase in the amount of energy collected through broadcasting, if it were

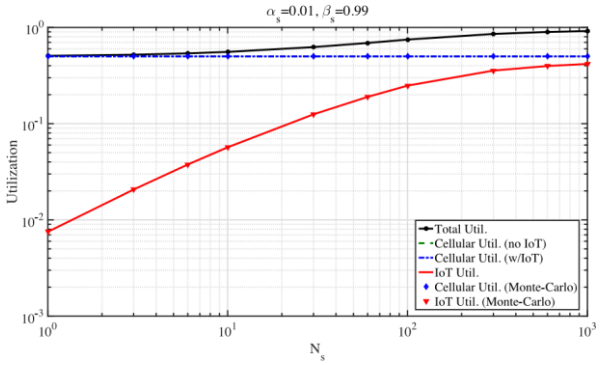

Figure 5: Cellular loT

Figure 5 illustrates the proportion of sensor nodes actively used for cellular, IoT, or full use. The outcomes of the Monte-Carlo calculations of cellular and IoT consumption are represented by blue diamonds or red triangles, respectively. When an opportunistic Internet of Things (IoT) network is present, the cell phone usage curve crosses over the baseline usage curve. Without it, the number of sensors in the Internet of Things would have stayed the same.

Due to retransmissions, the utilization curve for wireless connections in an impulsive IoT network is similar to the connections in the lack of IoT networking activity. The results reveal that as the failed detection probability rises and the maximum number of packet forwarding drops, the impact of the IoT network's existence on cellular network use grows. Also, with a 500 sensor network, the results show that the IoT system can achieve a cumulative utilization level of over 40% and a combined cellular but IoT channel utilization of over 90%. This demonstrates that such a procedure is possible and suitable in spectrally efficient or environmentally friendly IoT networks, including places.

We then focus on the impact that rising demand for SN traffic has on cellular or IoT usage rates by considering an IoT network that has a single SN. Fig. 6 depicts this idea visually. For a particular usage and pattern of cellular traffic (here, the wireless load is 50% with a 14 b 14 0:5), we find that there can be a maximum potential IoT utilization level. To meet the growing demand for SN transportation, p must drop.

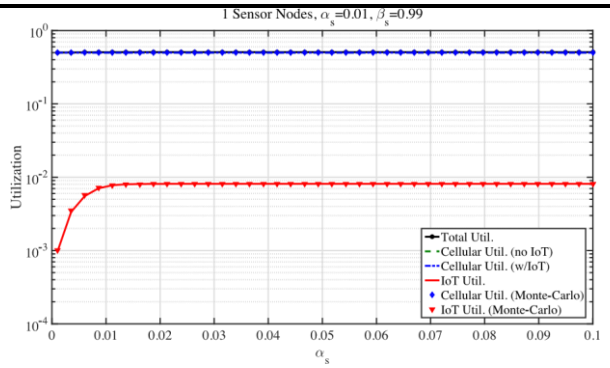

Figure 6: IoT network SN traffic parameter

Figure 6 shows the percentages of available capacity used by cell phones, Internet of Things devices, and the whole network. In this case, we have Ns 14 1 SN, b 14 0:5, a 14 0:5, and bs 14 0:99. Each point's p is optimized numerically.

Figure 7 depicts the relationship between Ns, as, and bs, and the cellular, IoT, & total usage rates of the cell membrane traffic parameter a. In this method, p is optimized numerically at each location. The outcomes of the Monte-Carlo calculations of cellular and IoT consumption are represented by blue diamonds or red triangles, respectively. It's important to remember that the two curves depicting cell use are too similar in all plots. They improved SN transmission power via energy transfer. However, the available spectrum is confined by the increased cellular traffic and the bare minimum spectrum for transfer of energy by CLH, over which the SN utilization level cannot be satisfied. This demonstrates the impracticality of high individual traffic volumes for SNs using RF energy harvesting or transfer, further substantiating the suitability of the system provided here for an IoT operating with very low or aperiodic single traffic loads.

We then look into cellular and IoT use as cellular traffic loads up. Fig. 6 depicts this idea visually. The accessible spectrum for the Internet of Things (IoT) network decreases as cellular traffic volumes rise. Since the usage of a single sensor node is constrained by limited available energy, the increase in the cellular traffic on the IoT utilization is insignificant when there is a detector node in the IoT networks (Figs. 7a and 7b). Sensor node traffic demand is as=as bs 14 1% in both Figs. 7a or 7b; however, the actual with as bs virtues in Fig. 7a portrays burstier traffic than those in Fig. 7b. Nevertheless, when there are various sensor networks in the Internet of Things network, the results change. We find that an increase in cellular traffic load has a detrimental effect on overall IoT utilization.

Finally, we look into how sensor performance affects utilization rates. Figure 8 shows a scatter plot of the percentage of time that a cellular or IoT network is in use versus the probability of delayed detection pMD for a range of values for the maximum number of cellular transmissions allowed, N. Since any decision boundary that yields

a pMD > 0:5 can be inverted to get a pMD 0:5 without losing applicability, pMD is swept among 0 and 0.5. The black horizontal dashed line in the illustration, which can be seen toward the right, depicts the utilization level of the cellular network in the absence of any IoT operations.

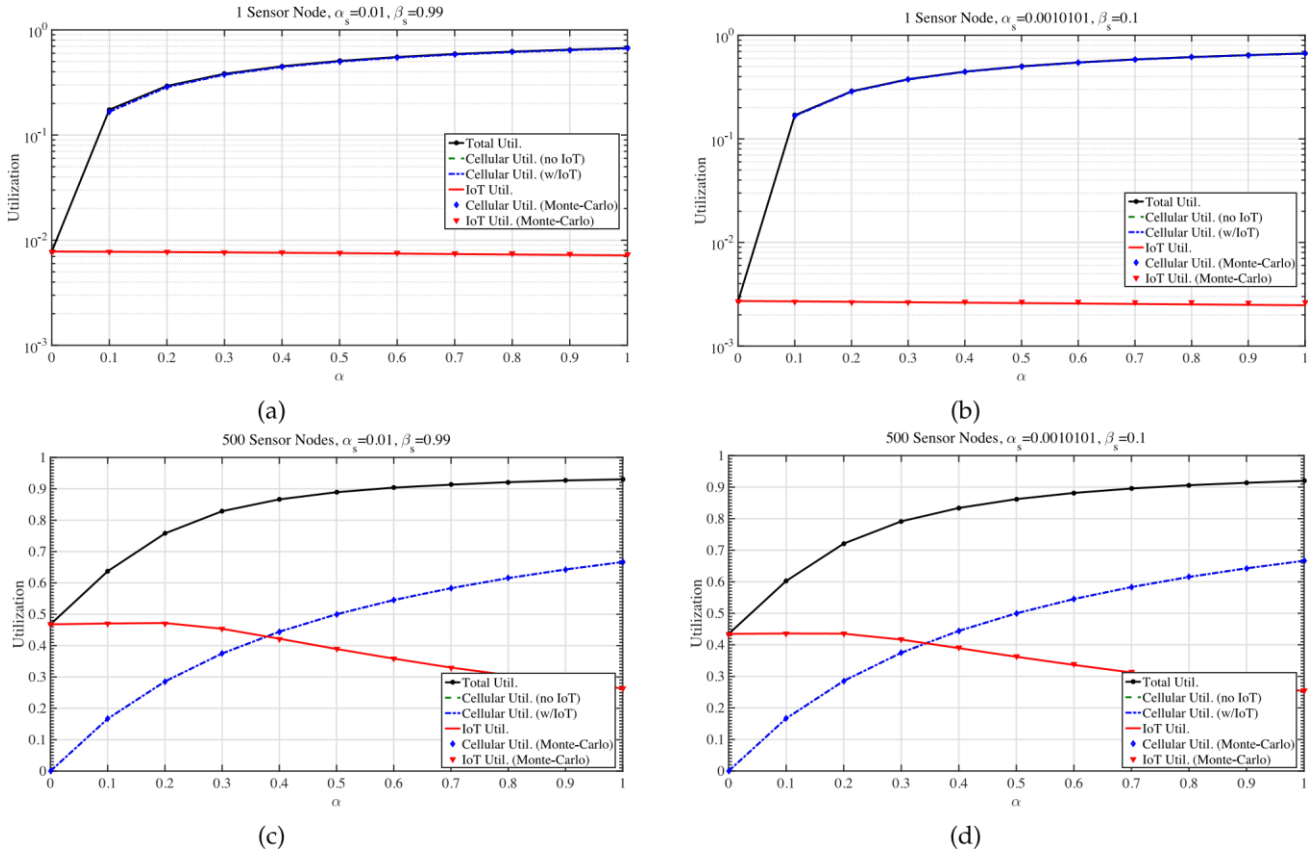

Figure 7: Cellular, loT, and total utilization levels

Even when the IoT network reaches around 40% utilization, the effect of IoT operations on the wireless network is negligible for low BMD or high N. The cellular network's retransmissions allow the vast majority of packets to be sent. The effect of the IoT networks on cellular consumption, however, becomes more evident as pMD rises and N falls. Since it is believed that packets that collide in both networks would be lost, IoT utilization decreases as pMD grows. However, for bigger pMD, IoT utilization rises with lower N, as the IoT connection makes better use of the available spectrum.

It has also been found that as pMD increases, the difference between the Markov Chain model's prediction of cellular network utilization levels and Monte-Carlo simulations grows. This is consistent with what was said in Section 4; the decoupling assumption begins to break down as the collision probability rises. However, the Markov Chain analysis or probability distributions do not significantly alter until pMD hits 0.3.

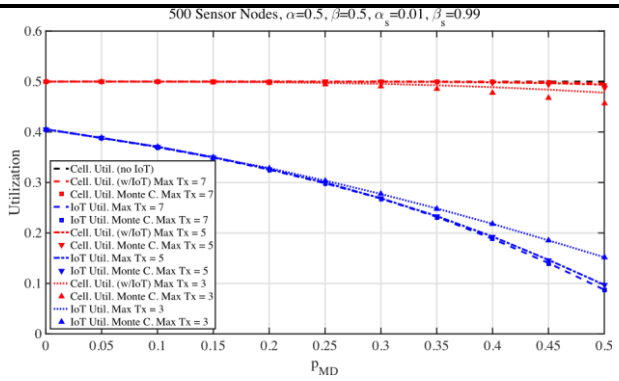

Figure 8: missed detection probability

Figure 8 displays the relationship between the maximum number of permissible cellular communications and the percentage of cells that are in use and the likelihood of a missed detection. Here, p is optimized numerically at every single position between zero and ninety-nine. The findings from Monte-Carlo simulations are remarkably close to the real thing. Therefore, we infer that the dissociation assumption is valid for realistic systems based on our simulation environment.

8.CONCLUSION

Our wireless IoT network is the first to propose collecting and transferring RF energy while also sharing its assessment of sample adequacy with other mobile networks. The proposed slot-synchronous IoT network consists of two nodes: a cluster head (CLH), including a stable power supply that performs imperfect recognition of the cellular data, and afterward randomly organizes energy nodes (SNs) for distribution. This process of energy transmission from the CLH towards the SNs occurs at random intervals during which the CLH is thought to be at rest. The SNs can then use this energy to power themselves, or they can continue to collect energy from the cellular network's transmissions. We demonstrate the interconnected nature of the spectrum, energy, information transfer, and power transmission in this framework. As the data volume increases, IoT network utilization rises even as individual utilizations fall. This is because of the distributed nature of the power transmission. We show that the proposed Internet of Things network is a viable 5G solution, especially for environmentally friendly, energy- or spectrally-efficient sensors operating the system with many nodes demanding mild and periodic traffic needs.

REFERENCES

1. J. Gubbi, R. Buyya, S. Marusic, and M. Palaniswami, "Internet of Things (IoT): A vision, architectural elements, and future directions," Future Generation Computer. Syst., vol. 29, no. 7, pp. 1645– 1660, Sep. 2013.
2. S. Amendola, R. Lodato, S. Manzari, C. Occhiuzzi, and G. Marrocco, "RFID technology for IoT-based personal healthcare in smart spaces," IEEE Internet Things J., vol. 1, no. 2, pp. 144–152, Apr. 2014.
3. N. Bui, A. P. Castellani, P. Casari, and M. Zorzi, "The internet of energy: A Web-enabled smart grid system," IEEE Netw., vol. 26, no. 4, pp. 39–45, Jul./Aug. 2012.
4. L. Foschini, T. Taleb, A. Corradi, and D. Bottazzi, "M2M-based metropolitan platform for IMS-enabled road traffic management in IoT," IEEE Commun. Mag., vol. 49, no. 11, pp. 50–57, Nov. 2011.
5. A. Zanella, N. Bui, A. Castellani, L. Vangelista, and M. Zorzi, "Internet of Things for smart cities," IEEE Internet Things J., vol. 1, no. 1, pp. 22–32, Feb. 2014.
6. K. Fleming, P. Waweru, M. Wambua, E. Modula, and L. Samuel, "Toward quantified small-scale farms in Africa," IEEE Internet Comput., vol. 20, no. 3, pp. 63–67, May/Jun. 2016.
7. M. T. Lazarescu, "Design of a WSN platform for long-term environmental monitoring for IoT applications," IEEE J. Emerging Sel. Topics Circuits Syst., vol. 3, no. 1, pp. 45–54, Mar. 2013.
8. H. S. Dhillon, H. Huang, and H. Viswanathan, "Wide-area wireless communication challenges for the Internet of Things," ArXiv e-prints, Apr. 2015. [Online]. Available: https://arxiv.org/abs/1504.03242
9. J. Gonzalez, "New 3GPP standard for IoT [Mobile Radio]," IEEE Veh. Technol. Mag., vol. 11, no. 1, pp. 14–20, Mar. 2016.
10. E. Borgia, "The Internet of Things vision: Key features, applications, and open issues," Comput. Commun., vol. 54, pp. 1–31, 2014.
11. R. V. Prasad, S. Devasenapathy, V. S. Rao, and J. Vazifehdan, "Reincarnation in the Ambiance: Devices and networks with energy harvesting," IEEE Commun. Surveys Tuts., vol. 16, no. 1, pp. 195–213, Jan.–Mar. 2014.
12. T. Rault, A. Bouabdallah, and Y. Challah, "Energy efficiency in wireless sensor networks: A top-down survey," Comput. Netw., vol. 67, no. 4, pp. 104–122, 2014.
13. S. Ulukus, et al., "Energy harvesting wireless communications: A review of recent advances," IEEE J. Sel. Areas Commun., vol. 33, no. 3, pp. 360–381, Mar. 2015.
14. S. Kitazawa, H. Ban, and K. Kobayashi, "Energy harvesting from ambient RF sources," in Proc. IEEE MTT-S Int. Microw. Workshop Series Innovative Wireless Power Transmiss.: Technol. Syst. Appl., May 2012, pp. 39–42.
15. X. Lu, P. Wang, D. Niyato, D. I. Kim, and Z. Han, "Wireless networks with RF energy harvesting: A contemporary survey," IEEE Commun. Surveys Tuts., vol. 17, no. 2, pp. 757–789, Apr.–Jun. 2015.

16. S. Lee, R. Zhang, and K. Huang, "Opportunistic wireless energy harvesting in cognitive radio networks," IEEE Trans. Wireless Commun., vol. 12, no. 9, pp. 4788–4799, Sep. 2013.
17. A. Osseiran, J. F. Monserrat, and P. Marsch, Eds., 5G Mobile and Wireless Communications Technology. Cambridge, U.K.: Cambridge Univ. Press, Jun. 2016.
18. Ericsson, "Ericsson mobility report on the pulse of the networked society," Nov. 2015. [Online]. Available: http://www.ericsson. Com/res/docs/2015/mobility-report/Ericsson-mobility-report Nov-2015.pdf
19. E. Hossain and M. Hasan, "5G cellular: Key enabling technologies and research challenges," IEEE Trans. Instrum. Meas., vol. 18, no. 3, pp. 11–21, Jun. 2015.
20. P. Kamalinejad, C. Mahapatra, Z. Sheng, S. Mirabbasi, V. C. M. Leung, and Y. L. Guan, "Wireless energy harvesting for the Internet of Things," IEEE Commun. Mag., vol. 53, no. 6, pp. 102–108, Jun. 2015.
21. M. Garlatova, G. Grebla, M. Cong, I. Kymissis, and G. Zussman, "Movers and shakers: Kinetic energy harvesting for the Internet of Things," IEEE J. Sel. Areas Commun., vol. 33, no. 8, pp. 1624– 1639, Aug. 2015.
22. L. Liu, R. Zhang, and K.-C. Chua, "Wireless information transfer with opportunistic energy harvesting," IEEE Trans. Wireless Commun., vol. 12, no. 1, pp. 288–300, Jan. 2013.
23. S. Luo, R. Zhang, and T. J. Lim, "Optimal save-then-transmit protocol for energy harvesting wireless transmitters," IEEE Trans. Wireless Commun., vol. 12, no. 3, pp. 1196–1207, Mar. 2013.
24. S. Yin, E. Zhang, L. Yin, and S. Li, "Optimal saving-sensing-transmitting structure in self-powered cognitive radio systems with wireless energy harvesting," in Proc. IEEE Int. Conf. Commun., Jun. 2013, pp. 2807–2811.
25. R. Zhang and C. K. Ho, "MIMO broadcasting for simultaneous wireless information and power transfer," IEEE Trans. Wireless Commun., vol. 12, no. 5, pp. 1989–2001, May 2013.
26. G. Zheng, Z. Ho, E. A. Jorswieck, and B. Ottersten, "Information and energy cooperation in cognitive radio networks," IEEE Trans. Signal Process., vol. 62, no. 9, pp. 2290–2303, May 2014.
27. M.-L. Ku, Y. Chen, and K. J. R. Liu, "Data-driven stochastic models and policies for energy harvesting sensor communications," IEEE J. Sel. Areas Commun., vol. 33, no. 8, pp. 1505–1520, Aug. 2015.
28. W. H. R. Chan, et al., "Adaptive duty cycling in sensor networks with energy harvesting using continuous-time Markov chain and fluid models," IEEE J. Sel. Areas Commun., vol. 33, no. 12, pp. 2687–2700, Dec. 2015.
29. D. T. Hoang, D. Niyato, P. Wang, D. I. Kim, and S. Member, "Opportunistic channel access and RF energy harvesting in cognitive radio networks," IEEE J. Sel. Areas Commun., vol. 32, no. 11, pp. 2039–2052, Nov. 2014.

30. D. T. Hoang, D. Niyato, P. Wang, and D. I. Kim, "Performance optimization for cooperative multiuser cognitive radio networks with RF energy harvesting capability," IEEE Trans. Wireless Commun., vol. 14, no. 7, pp. 3614–3629, Jul. 2015.
31. S. Yin, Z. Qu, and S. Li, "Achievable throughput optimization in energy harvesting cognitive radio systems," IEEE J. Sel. Areas Commun., vol. 33, no. 3, pp. 407–422, Mar. 2015.
32. J. Kim and G. Hwang, "Stability analysis of multi-channel cognitive radio networks based on decoupling approach," in Proc. 7th Int. Conf. Ubiquitous Future Netw., 2015, pp. 645–650.
33. N. Tadayon and S. A€ıssa, "Multi-channel cognitive radio networks: Modeling, analysis and synthesis," IEEE J. Sel. Areas Commun., vol. 32, no. 11, pp. 2065–2074, Nov. 2014.
34. N. Tadayon and S. A€ıssa, "Modeling and analysis framework for multi-interface multi-channel cognitive radio networks," IEEE Trans. Wireless Commun., vol. 14, no. 2, pp. 935–947, Feb. 2015.
35. T. Yuck and H. Arslan, "A survey of spectrum sensing algorithms for cognitive radio applications," IEEE Commun. Surveys Tuts., vol. 11, no. 1, pp. 116–130, Jan.–Mar. 2009.
36. M. Sahin, I. Guvenc, M. R. Jeong, and H. Arslan, "Handling CCI and ICI in OFDMA femtocell networks through frequency scheduling," IEEE Trans. Consum.Electron., vol. 55, no. 4, pp. 1936–1944, Nov. 2009.
37. S. Geirhofer and L. Tong, "Dynamic spectrum access in the time domain: Modeling and exploiting white space," IEEE Commun. Mag., vol. 45, no. 5, pp. 66–72, May 2007.
38. M. Levorato, U. Mitra, and M. Zorzi, "Cognitive interference management in retransmission-based wireless networks," IEEE Trans. Inf. Theory, vol. 58, no. 5, pp. 3023–3046, May 2012.
39. M. Levorato, S. Firouzabadi, and A. Goldsmith, "A learning framework for cognitive interference networks with partial and noisy observations," IEEE Trans. Wireless Commun., vol. 11, no. 9, pp. 3101–3111, Sep. 2012.
40. G. Bianchi, "Performance analysis of the IEEE 802.11 distributed coordination function," IEEE J. Sel. Areas Commun., vol. 18, no. 3, pp. 535–547, Mar. 2000.
41. A. Kumar, E. Altman, D. Miorandi, and M. Goyal, "New insights from a fixed-point analysis of single-cell IEEE 802.11 WLANs," IEEE/ACM Trans. Netw., vol. 15, no. 3, pp. 588–601, Jun. 2007.
42. V. Ramaiyan, A. Kumar, and E. Altman, "Fixed point analysis of single-cell IEEE 802.11e WLANs: Uniqueness, multistability, and throughput differentiation," ACM SIGMETRICS Performance Eval. Rev., vol. 33, no. 1, pp. 109–120, 2005.

43. G. Sharma, A. Ganesh, and P. Key, "Performance analysis of contention-based medium access control protocols," IEEE Trans. Inf. Theory, vol. 55, no. 4, pp. 1665–1682, Apr. 2009.
44. J.-w. Cho, J.-Y. Le Boudec, and Y. Jiang, "On the asymptotic validity of the decoupling assumption for analyzing 802.11 MAC protocol," IEEE Trans. Inf. Theory, vol. 58, no. 11, pp. 6879–6893, Nov. 2012.
45. A. Leon-Garcia, Probability, Statistics, & Random Processes for Electrical Engineering, 3rd ed. Englewood Cliffs, NJ, USA: Prentice Hall, 2007.